Supplementary information

Dicyclohexylurea derivatives of amino acids as dye absorbent organogels and anion sensors

Karabi Roy,[1] Suvankar Ghosh,[2] Monikha Chetia[1], Priyadarshi Satpati[2*]and Sunanda Chatterjee[1*]

1. Department of Chemistry,

   Indian Institute of Technology, Guwahati

   Guwahati, Assam, India 781039.

   Email: sunanda.c@iitg.ac.in

   Telephone: 0361-2583310

   Fax:

2. Department of Biosciences and Bioengineering

   Indian institute of technology, Guwahati,

   Guwahati, Assam, India 781039.

   Email: psatpati@iitg.ac.in

   Telephone:0361-2583205

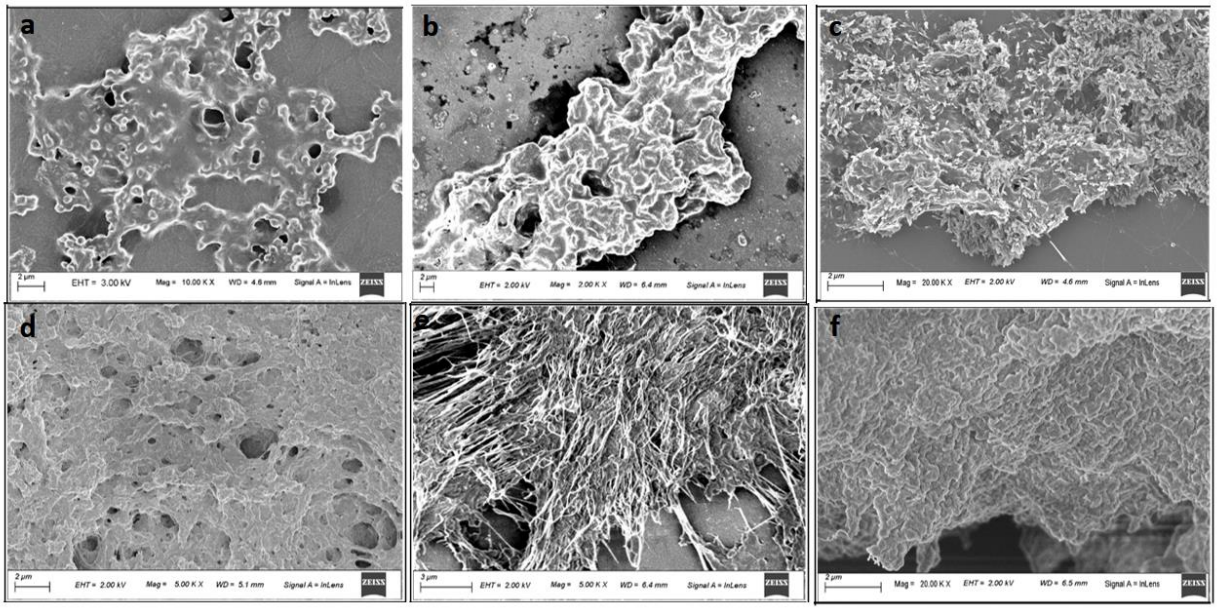

Figure S1: FESEM of M1-M3 a-c) in solution at 10mM concentration in 1,2 DCB and d-f) in gel state.

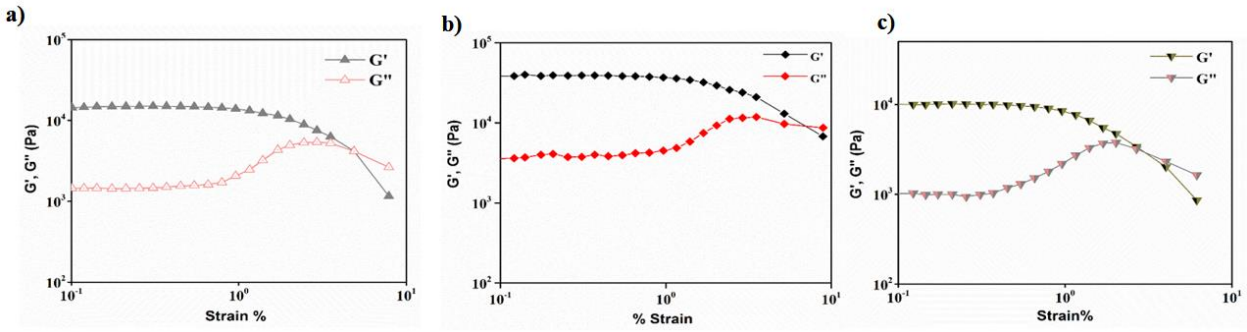

Figure S2: Rheology of xerogels of a) M1, b) M2 and c) M3 as a function of % strain.

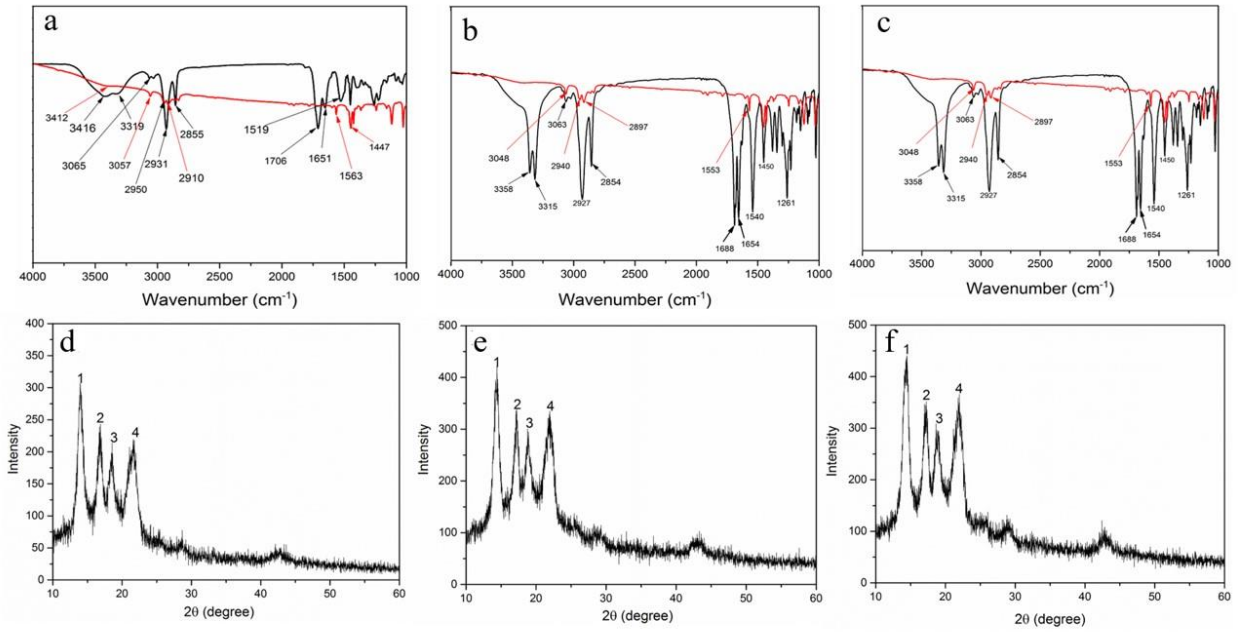

Figure S3: a-c) Comparison of the IR spectra of M1-M3 in powdered (black) and xerogel (red) state. d-f) PXRD pattern of M1-M3 in their xerogel state prepared from 1,2 DCB.

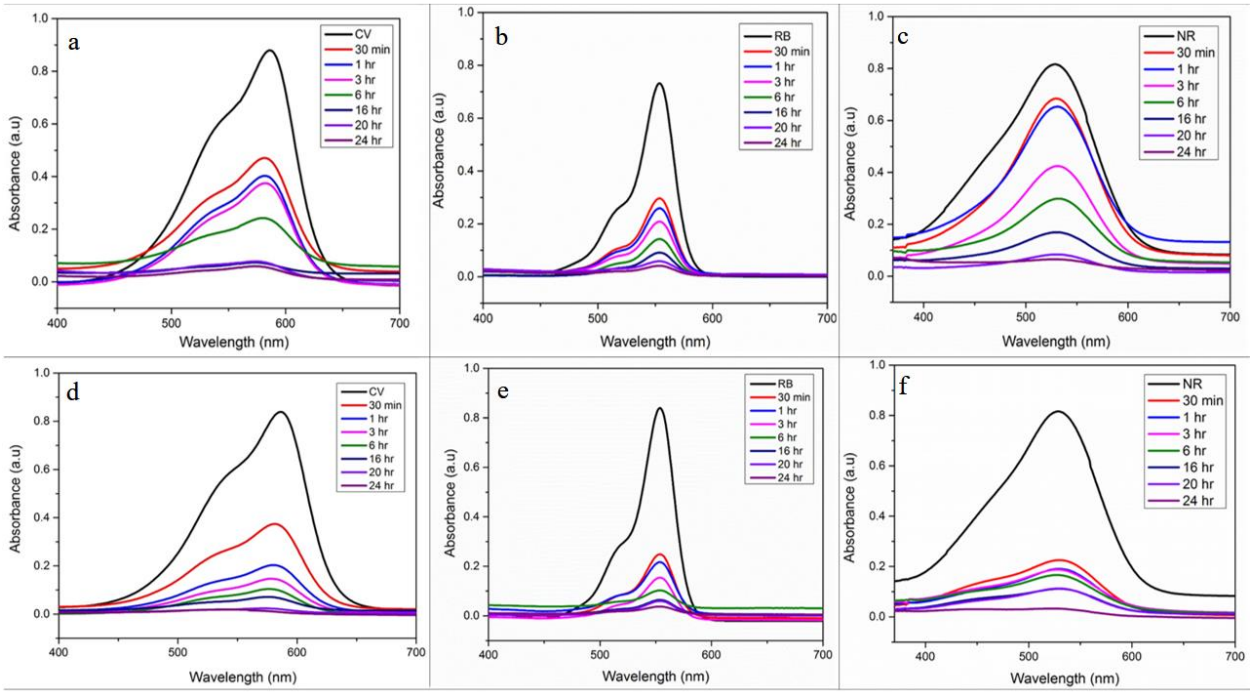

Figure S4: Absorption of dyes by organogels studied by UV spectroscopy. Time dependent absorption spectra of the supernatant solution containing CV (a,d),RB (b,e) and NR (c,f) incubated with organogels formed by M2 and M3 respectively in 1,2 DCB.

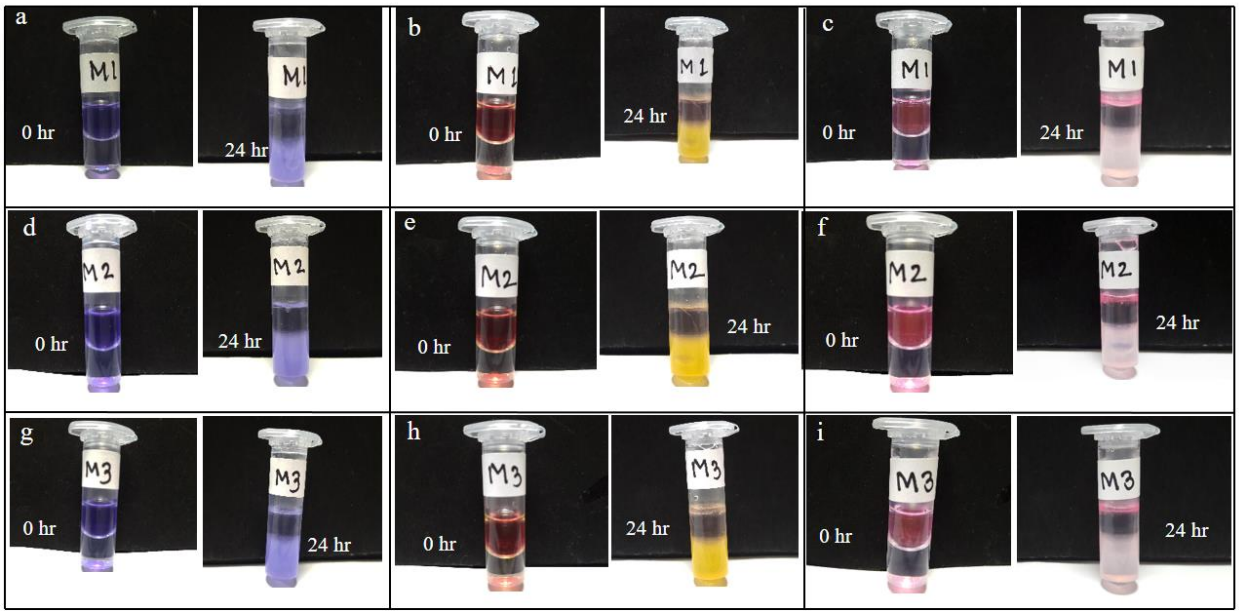

Figure S5: Absorption of dyes CV (a, d, g), RB (b, e, h), NR(c, f, i) by the organogels M1, M2 and M3 respectively, in 1,2 DCB at time t = 0 and t = 24hrs. LMWG in 1,2 DCB (colorless) is mixed with aqueous solution of dye, mixture is heated and cooled subsequently at t = 0 hrs. Within t = 24hrs, the gels turn colored due to dye absorption.

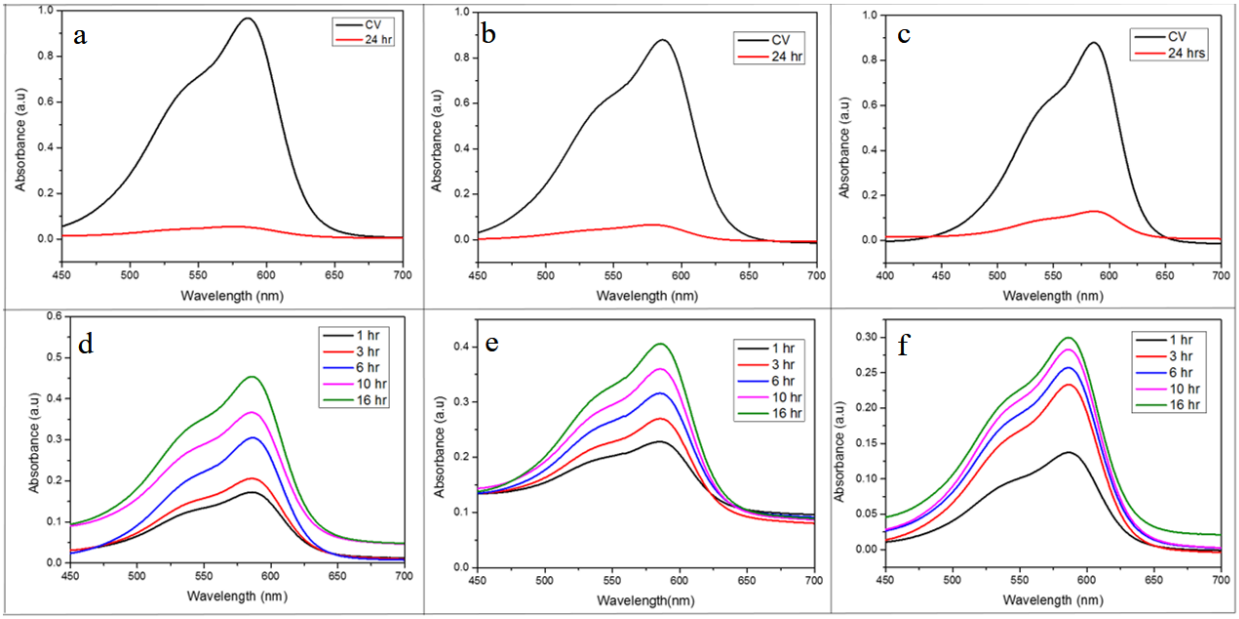

Figure S6: Reusability of organogels in dye absorption. a-c) UV-Vis graph showing CV (40 µM) loading after 24 hrs. in cycles 1-3 in the organogel formed from M1 in 1,2 DCB.d-f)UV-Vis

graph showing time dependent CV release from the M1 organogel in the three subsequent cycles.

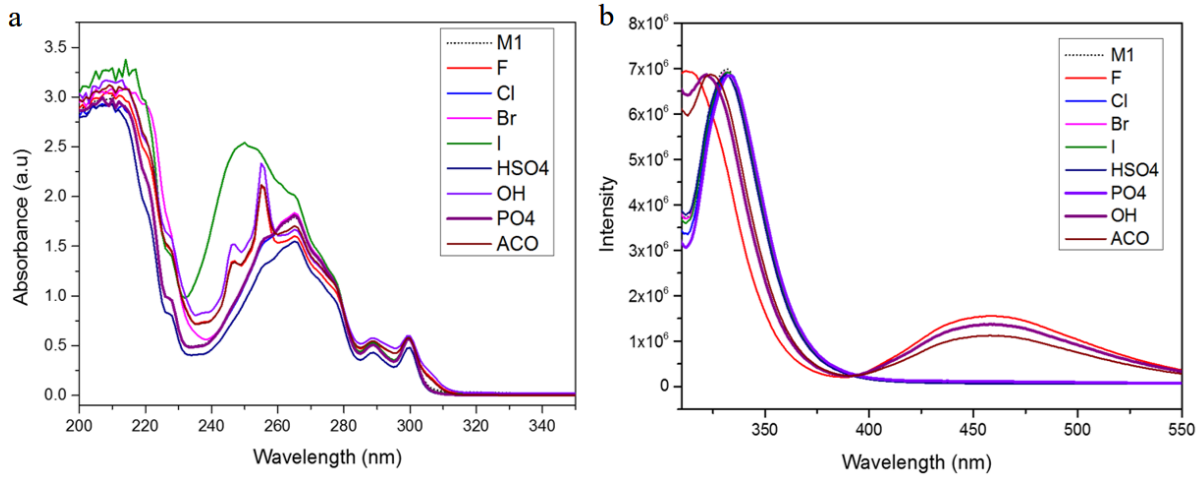

Figure S7: a) UV-Vis and b) Fluorescence spectra showing anion sensing of M1 in ACN (0.1 mM) for different anions (0.1 mM).

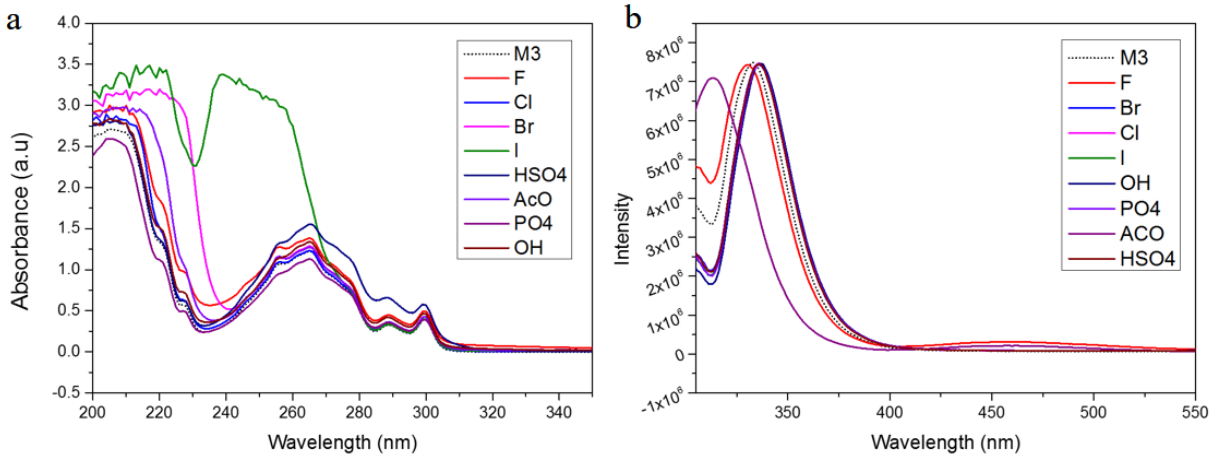

Figure S8: a) UV-Vis and b) Fluorescence spectra showing anion sensing of M3 in ACN (0.1 mM) for different anions (0.1 mM).

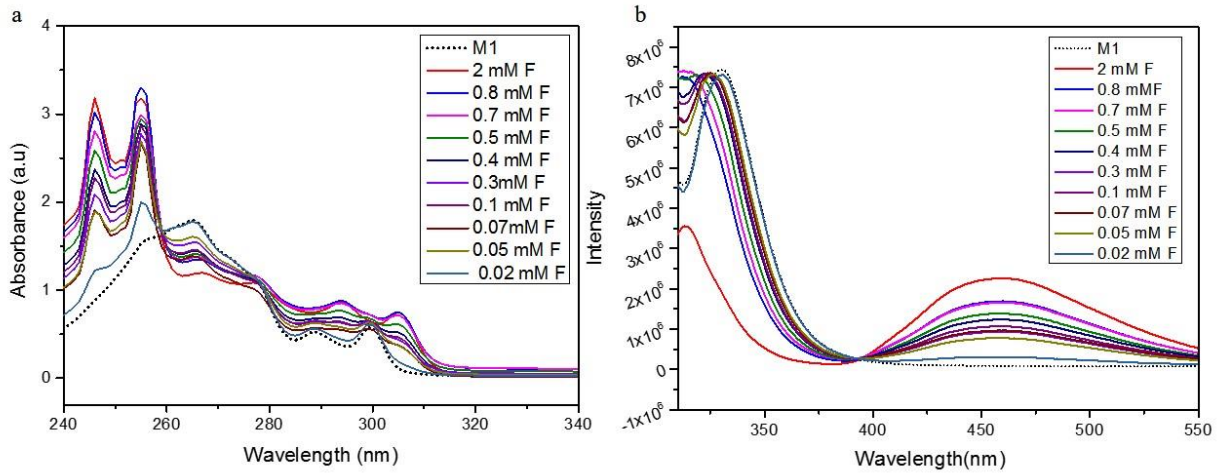

Figure S9: Fluoride ion concentration (0.02 -2 mM) dependent a) UV-Vis and b) Fluoresence spectra of M1 in ACN (0.1 mM)

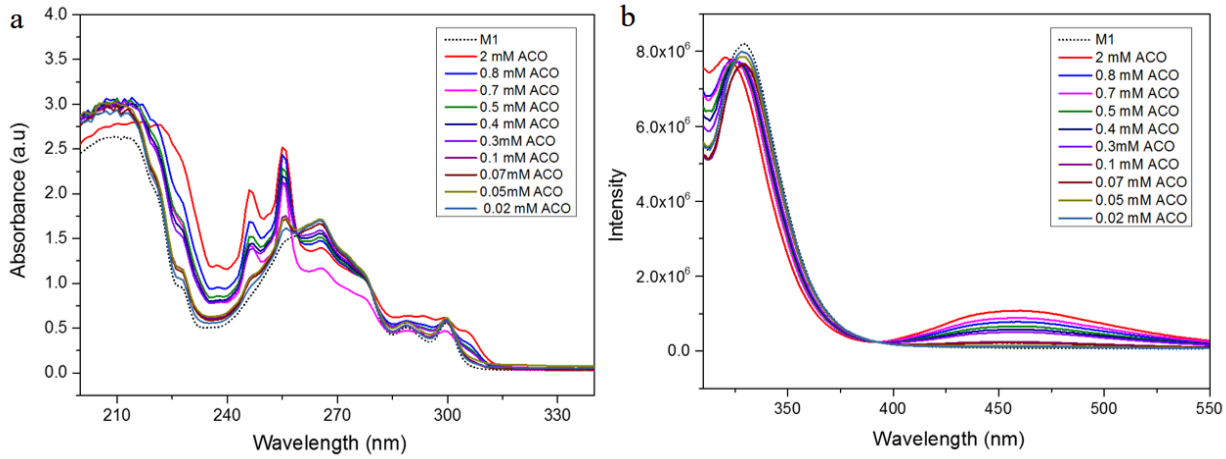

Figure S10: Acetate ion concentration (0.02 -2 mM) dependent a) UV-Vis and b) Fluorescence spectra of M1 in ACN (0.1 mM).

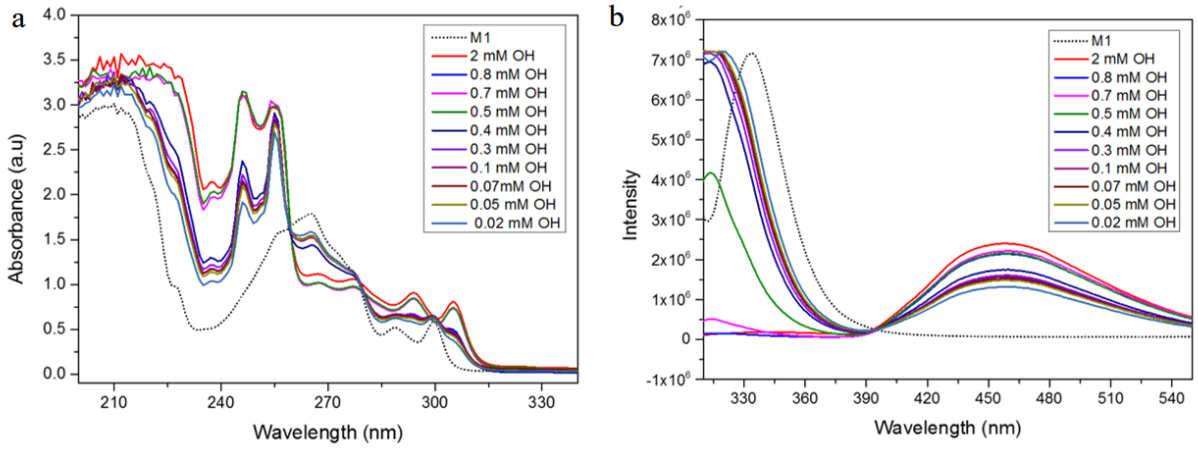

Figure S11: Hydroxide ion concentration (0.02 -2 mM) dependent a) UV-Vis and b) Fluorescence spectra of M1 in ACN (0.1 mM).

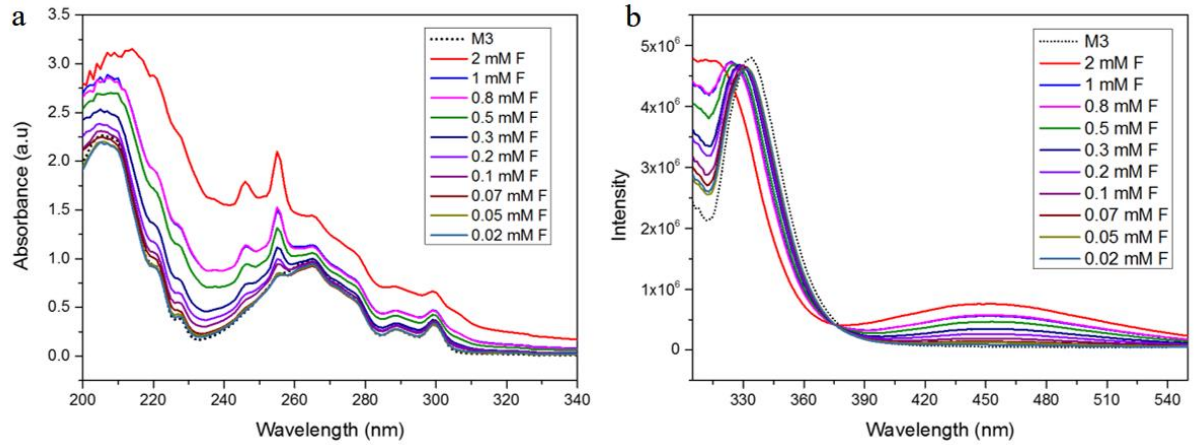

Figure S12: Fluoride ion concentration (0.02 -2 mM) dependent a) UV-Vis and b) Fluorescence spectra of M3 in ACN (0.1 mM).

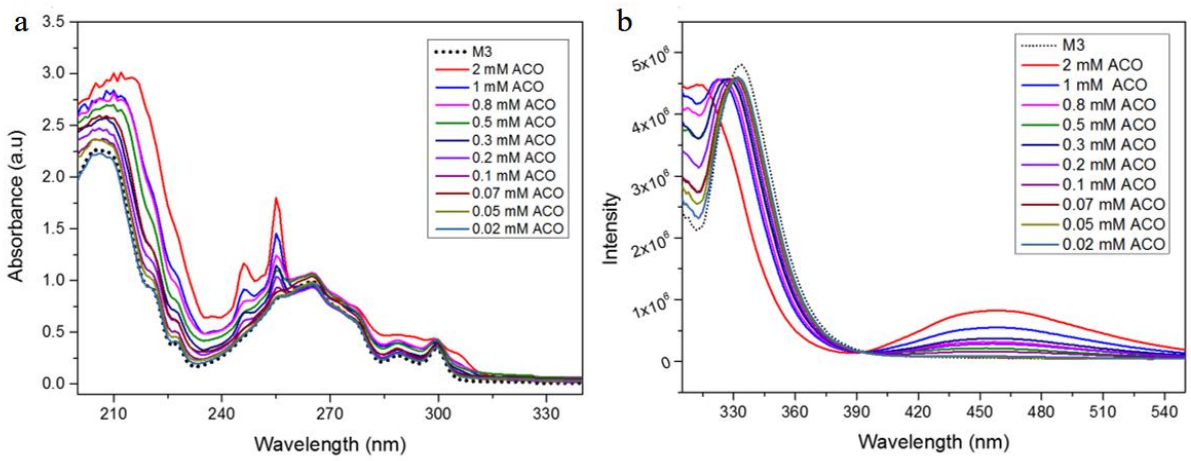

Figure S13: Acetate ion concentration (0.02 -2 mM) dependent a) UV-Vis and b) Fluorescence spectra of M3 in ACN (0.1 mM)

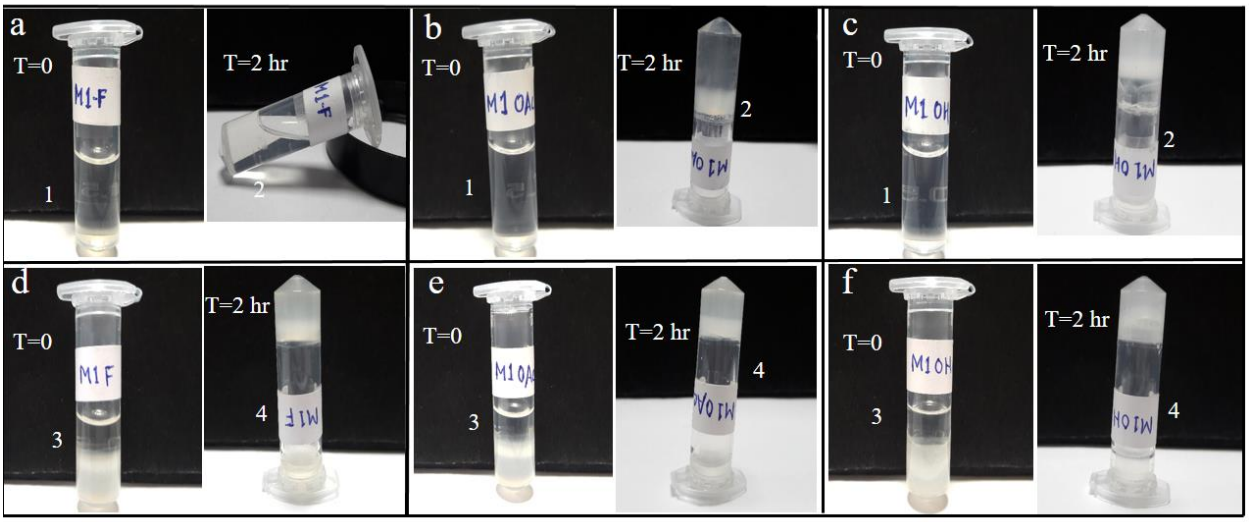

Figure S14: Effect of Fluoride, acetate and hydroxide ions on the (a-c) formation and (d-f) disruptionof organogels formed from M1. Only fluoride prevents formation of organogel, while none of the anions cause gel to disrupt.

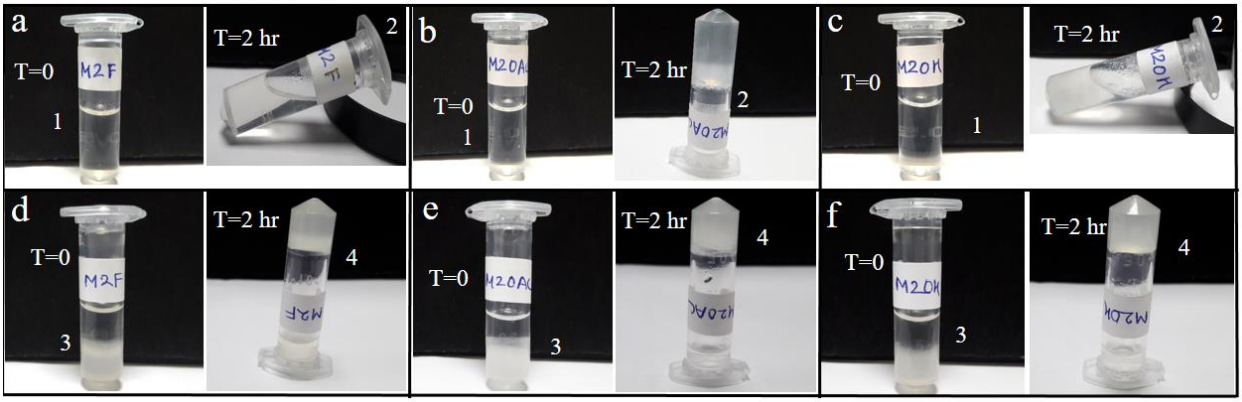

Figure S15:Effect of Fluoride, acetate and hydroxide ions on the (a-c)formation and (d-f) disruption of organogels formed from M2. Fluoride and hydroxide prevents formation of organogel, while none of the anions cause gel to disrupt.

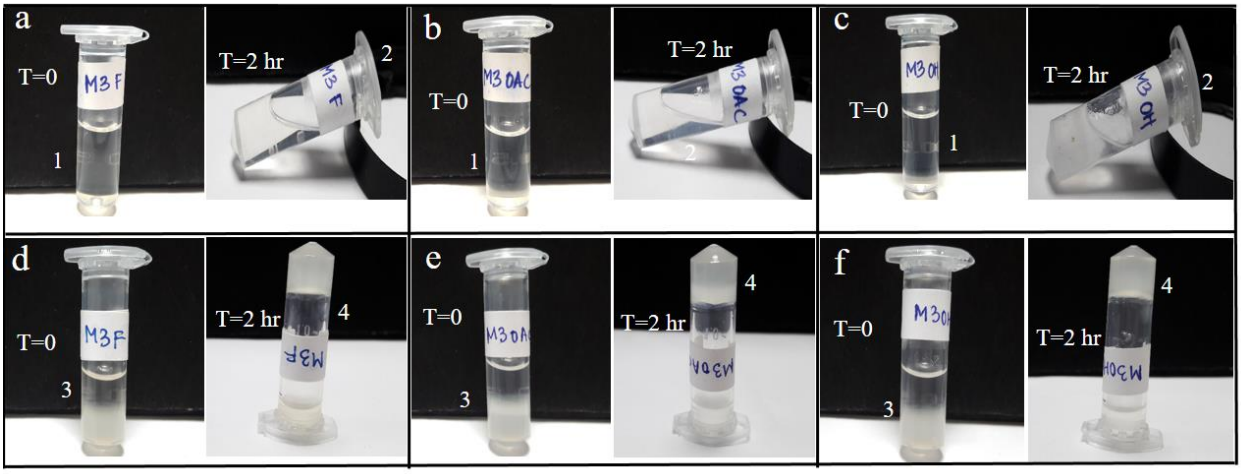

Figure S16: Effect of Fluoride, acetate and hydroxide ions on the (a-c) formation and (d-f) disruption of organogels formed from M3. All the three anions prevent formation of organogel, while none of the anions cause gel to disrupt.

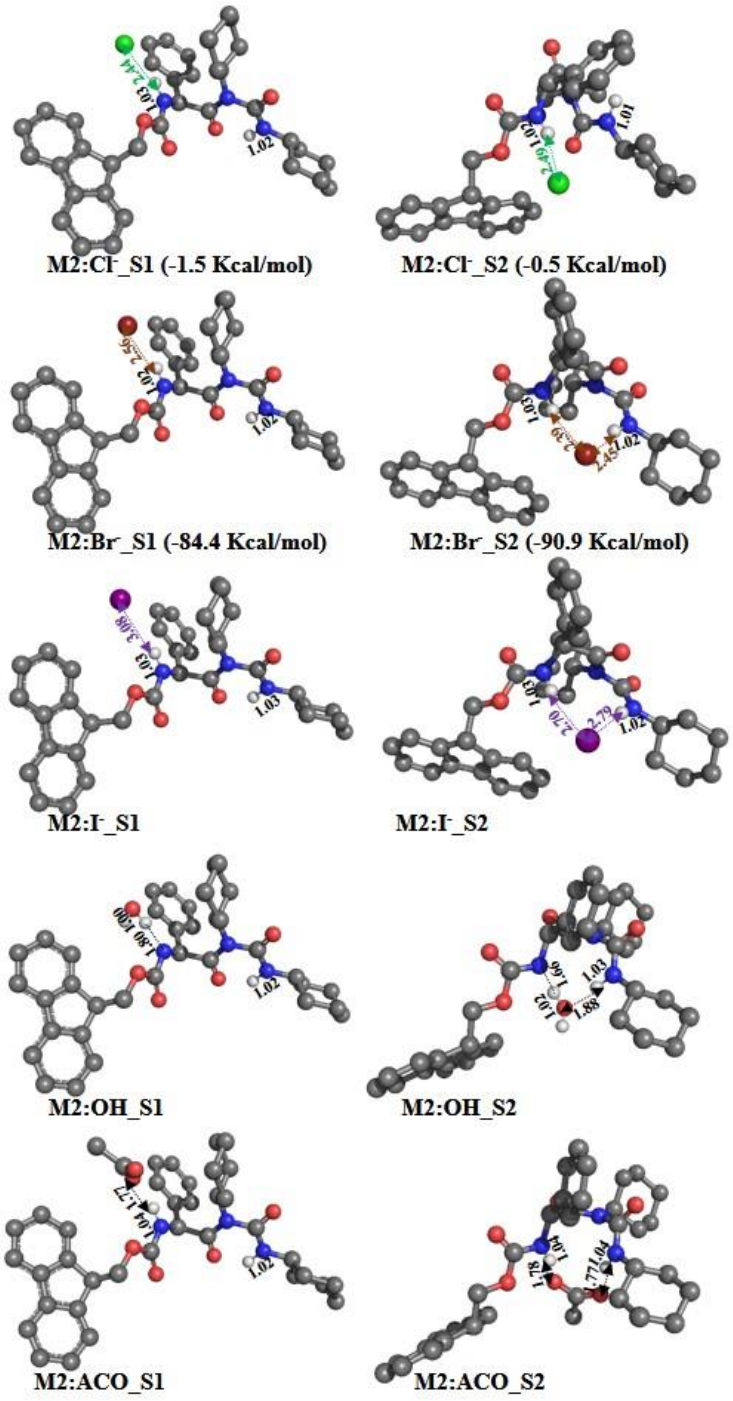

Fig S17: The optimized geometries of M2:X^- (X = Cl, Br, I, OH, OAc)

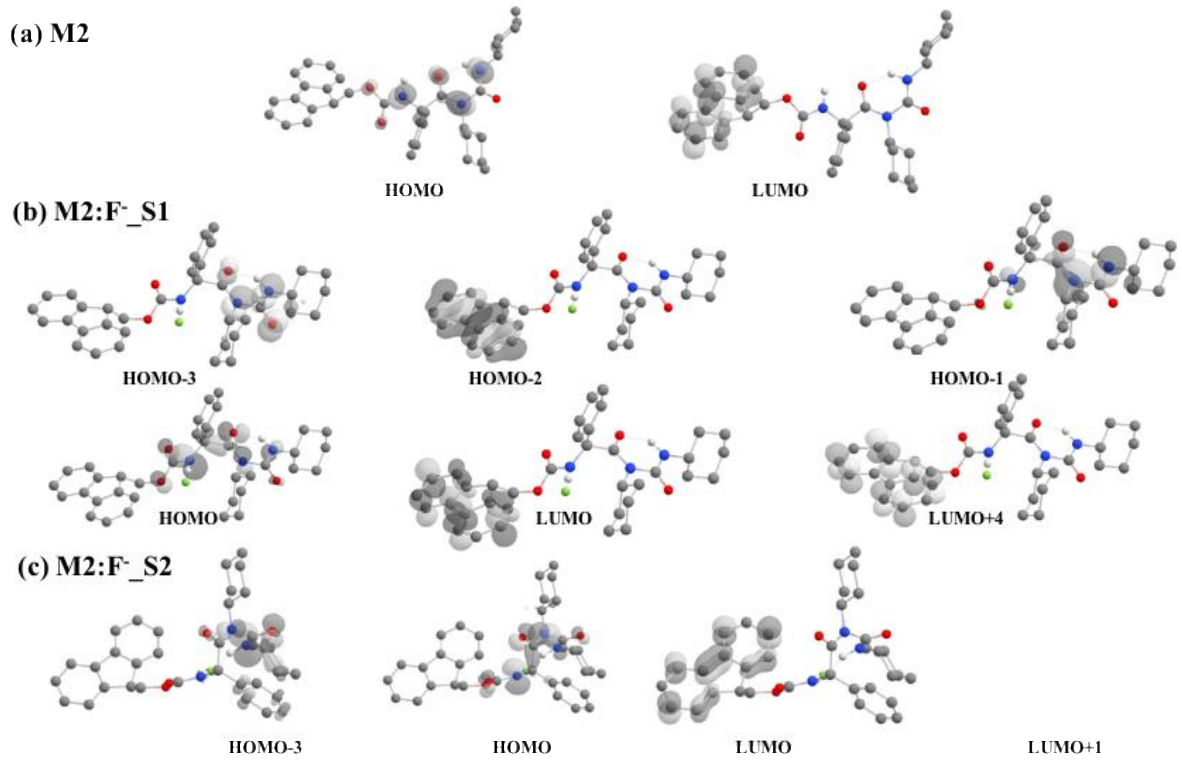

Figure S18: Molecular orbitals (MO) involved in characteristic UV-Vis absorption peaks (a) M2 (b) M2:F⁻_S1 (c) M2:F⁻_S2.

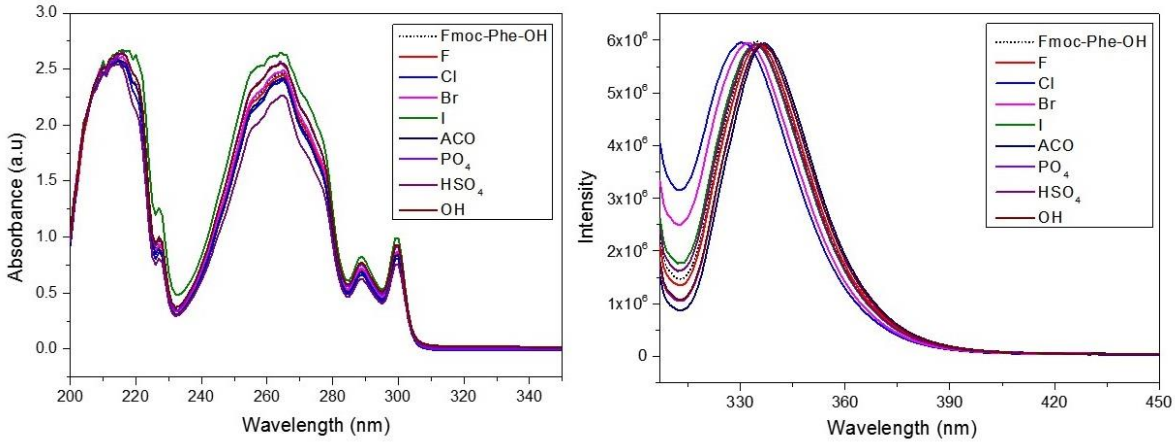

Figure S19: Anion sensing abilities of Fmoc-Phe-OH

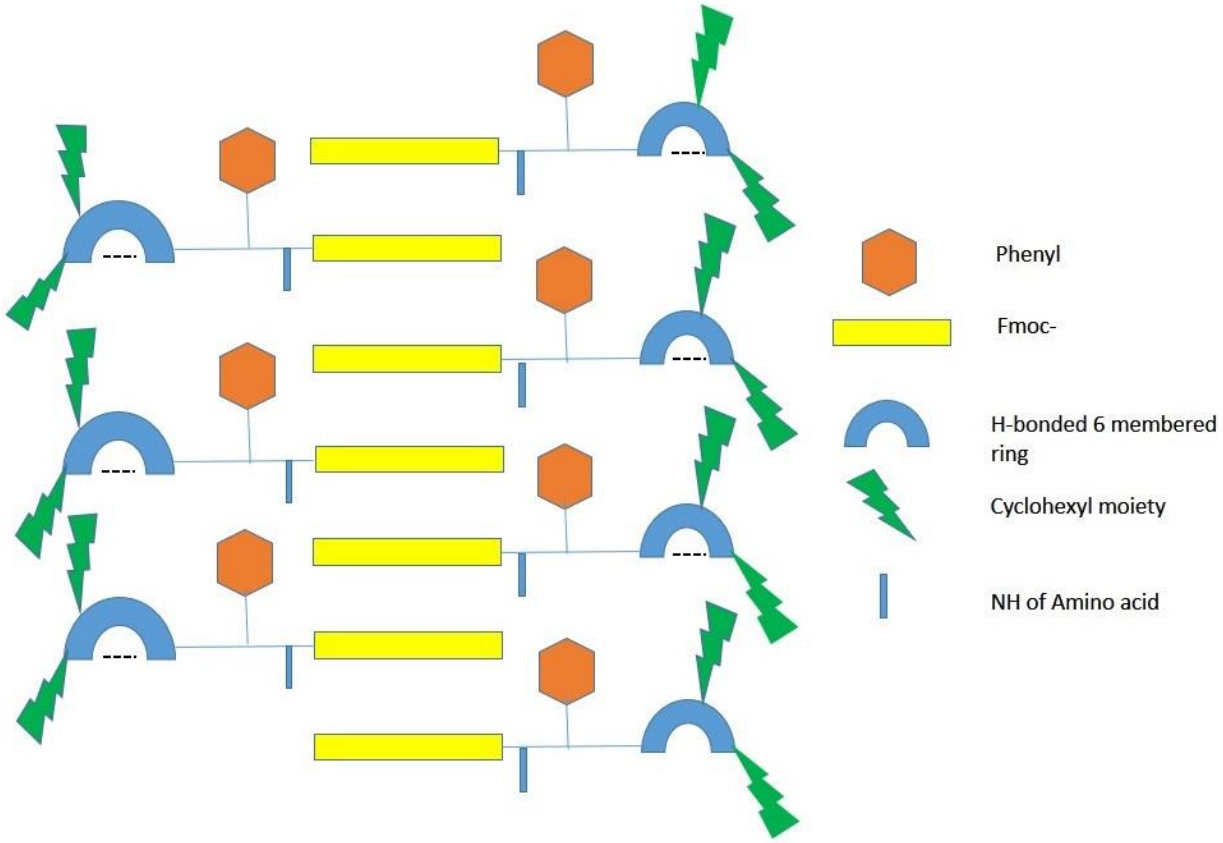

Figure S20: Schematic for self-assembly of the organogels from M1-M3.

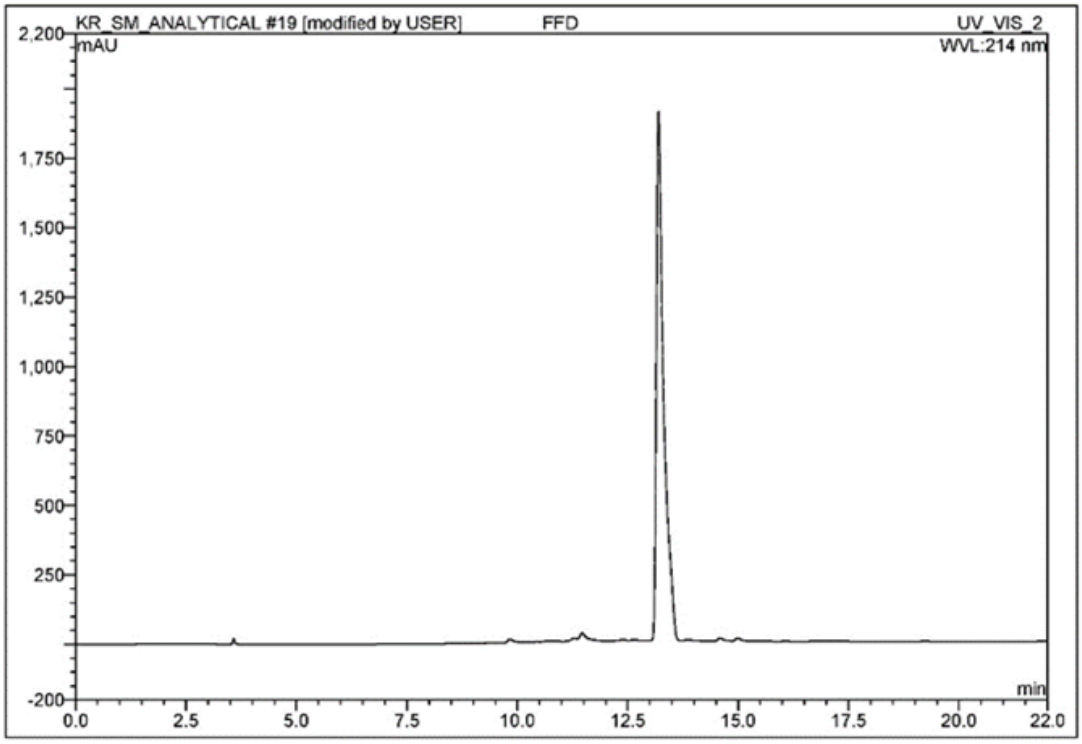

Figure S21: Analytical HPLC trace of M1.

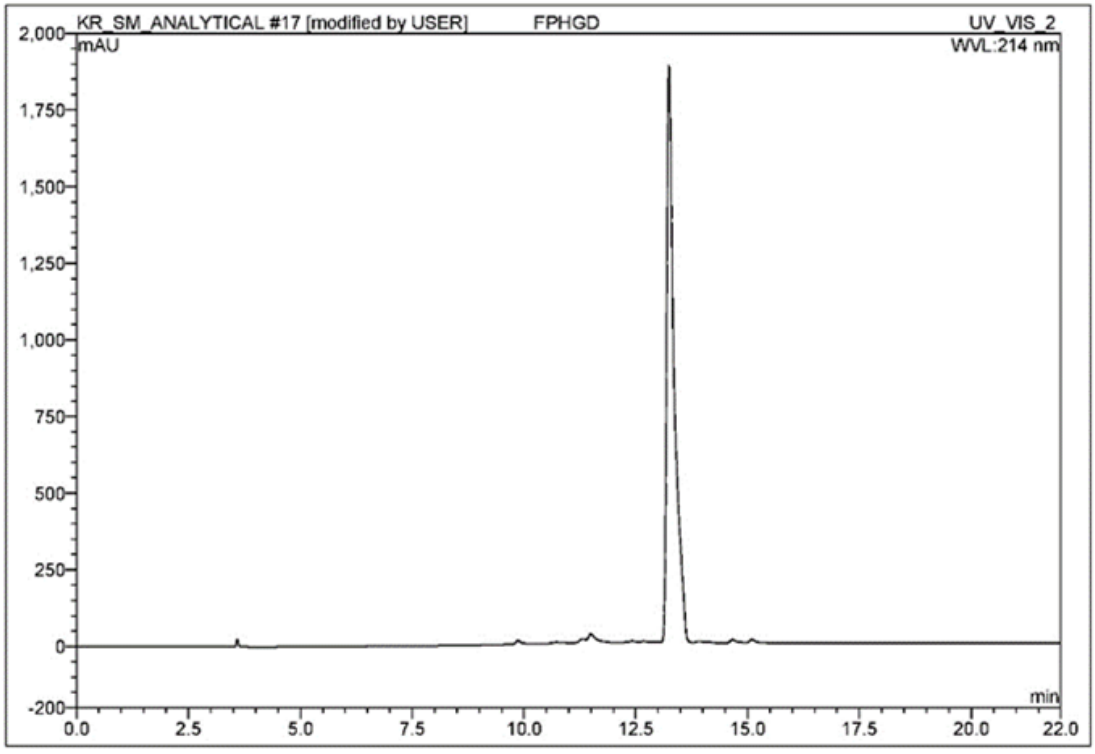

Figure S22: Analytical HPLC trace of M2

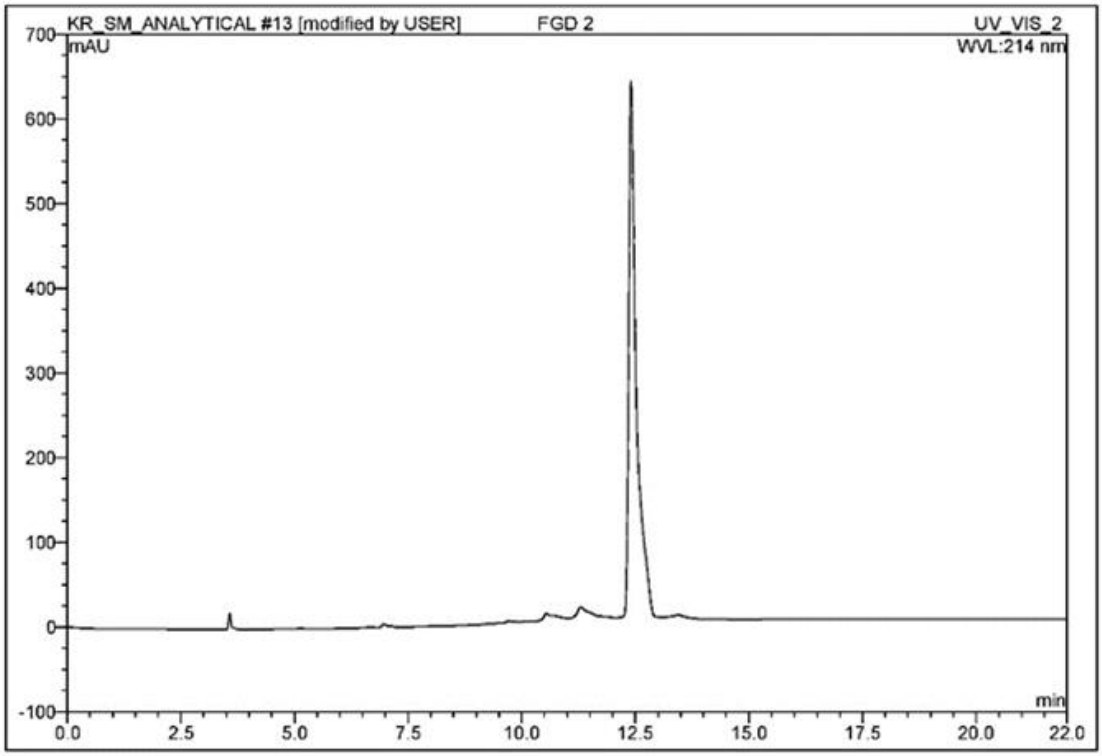

Figure S23: Analytical HPLC trace of M3.

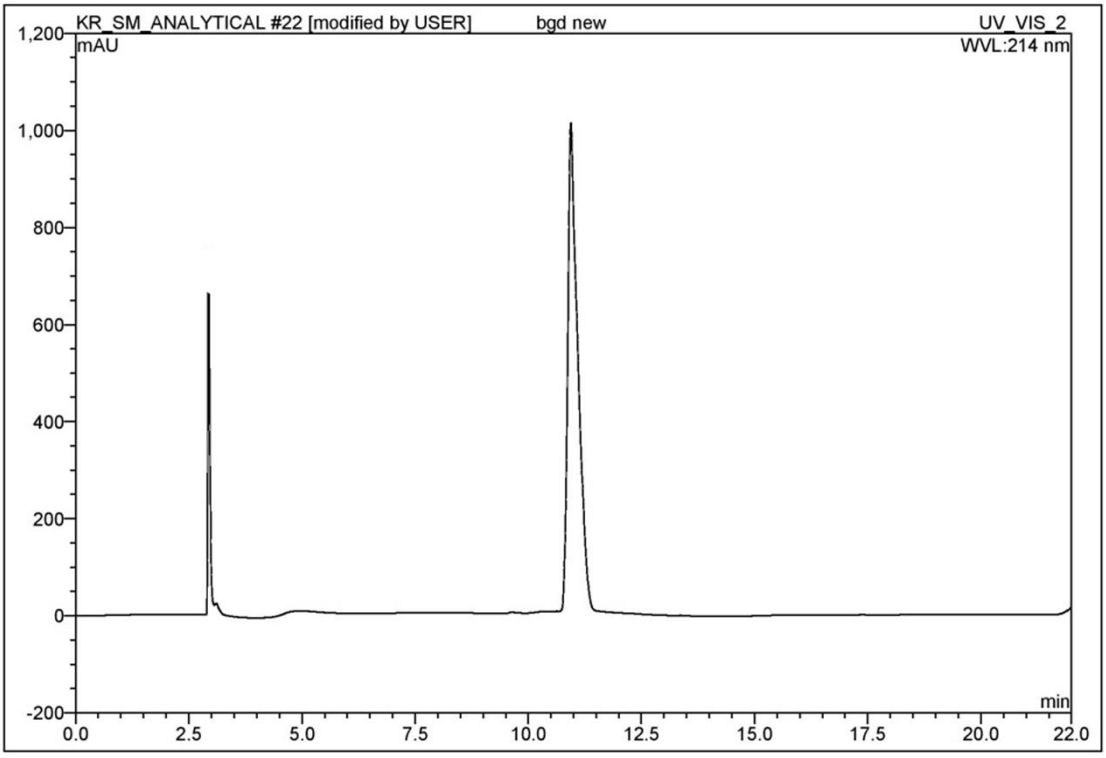

Figure S24: Analytical HPLC trace of M4.

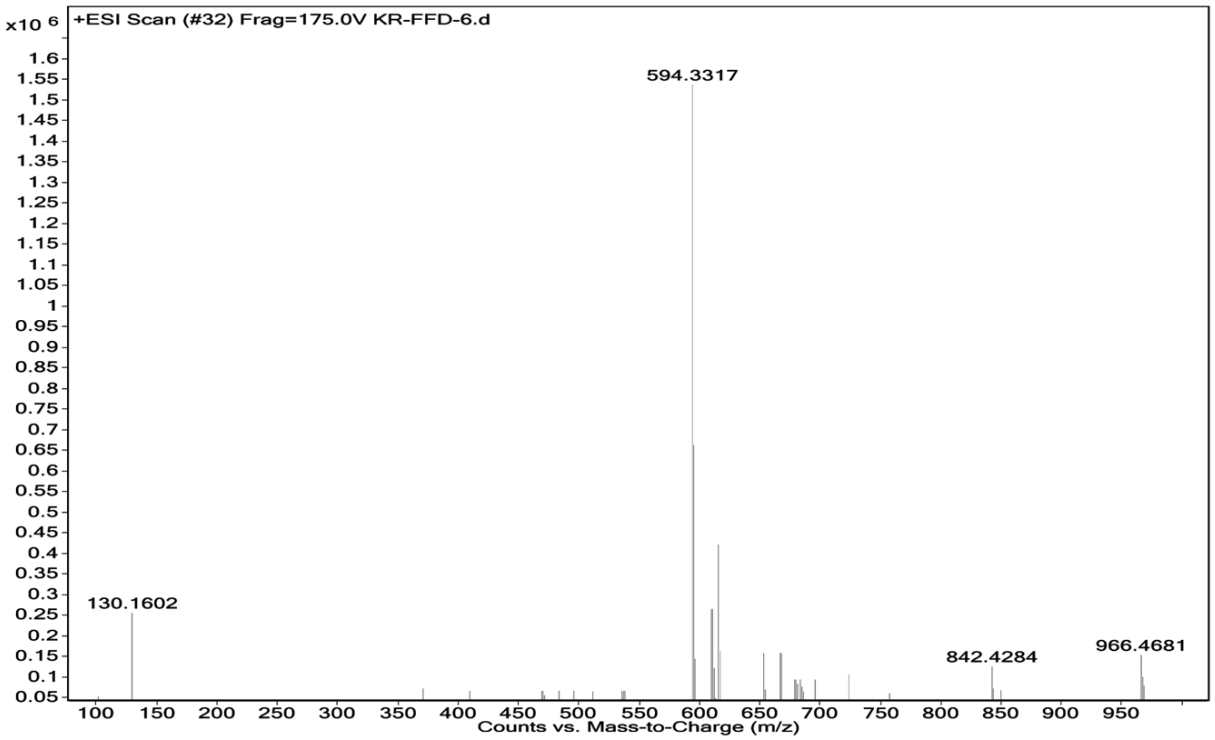

Figure S25: ESI-HRMS of M1. Mass calc. for M1: $(M+H)^+$ =594.3287 Da; Mass Obs.: $(M+H)^+$=594.3317 Da

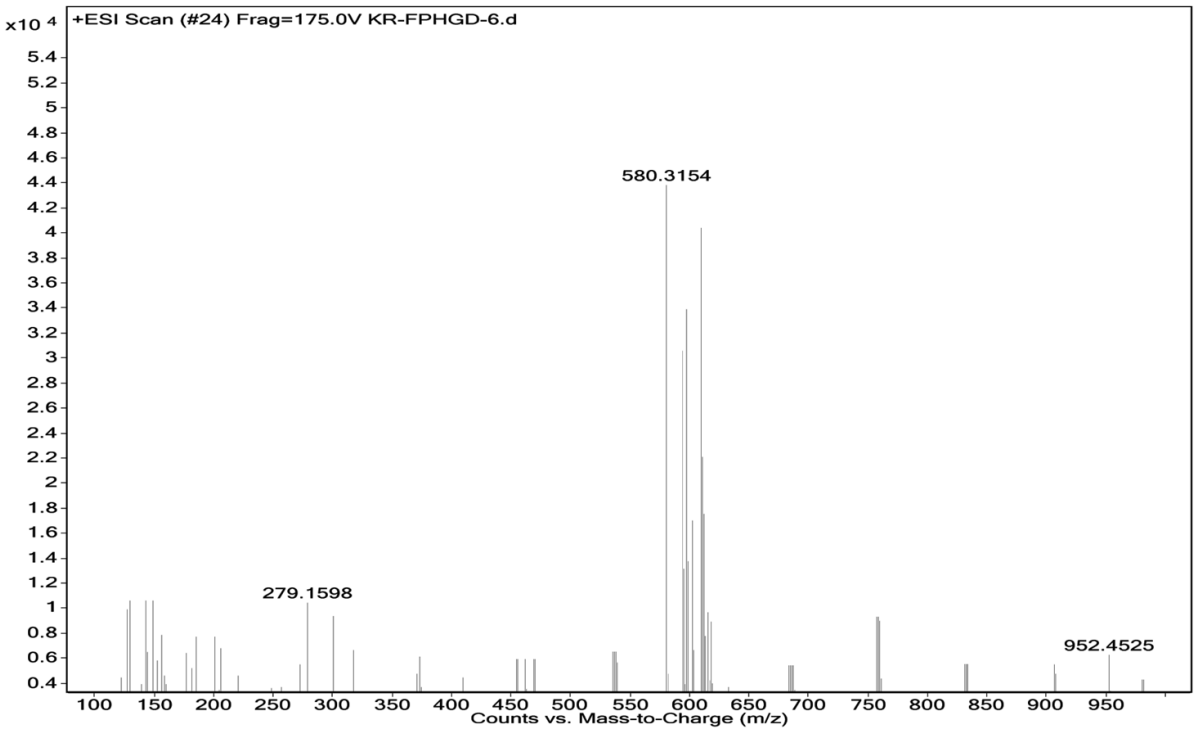

Figure S26: ESI-HRMS of M2. Mass calc. for M2: $(M+H)^+$ =580.3131 Da; Mass obs.: $(M+H)^+$=580.3154 Da

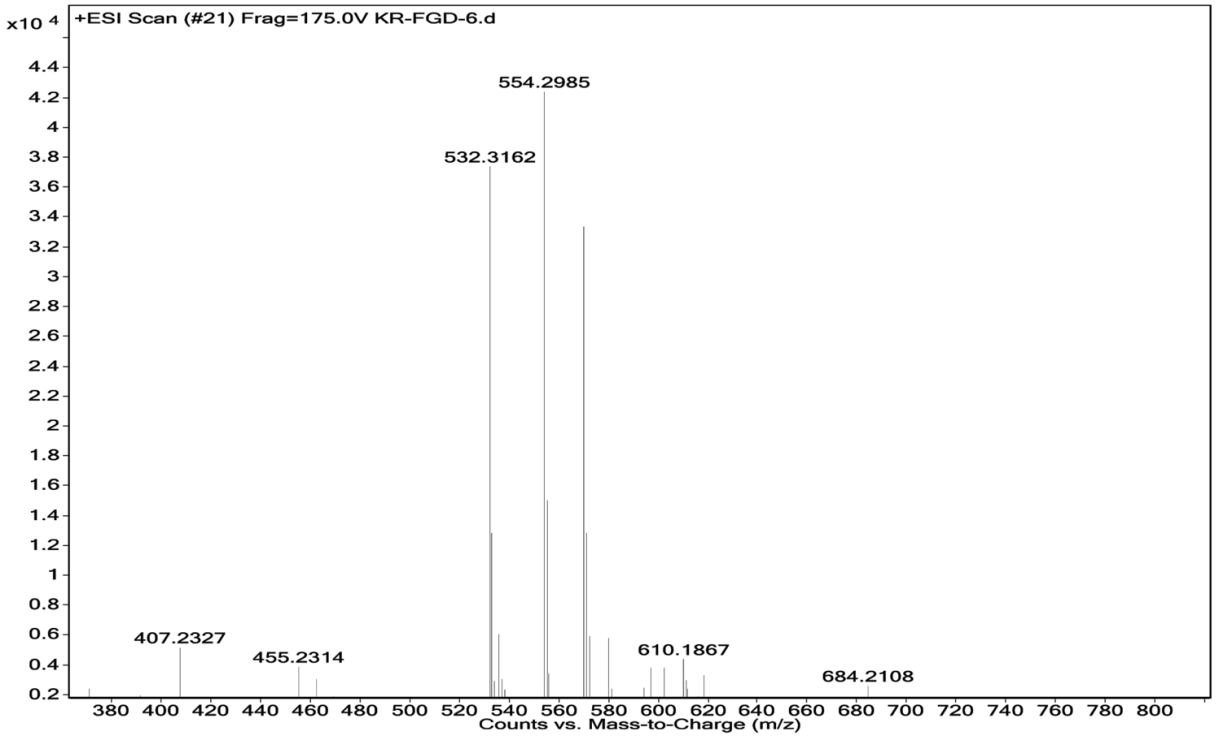

Figure S27: ESI-HRMS of M3. Mass calc. for M3: $(M+H)^+$=532.3131 Da; Mass obs.: $(M+H)^+$=532. 3162 Da.

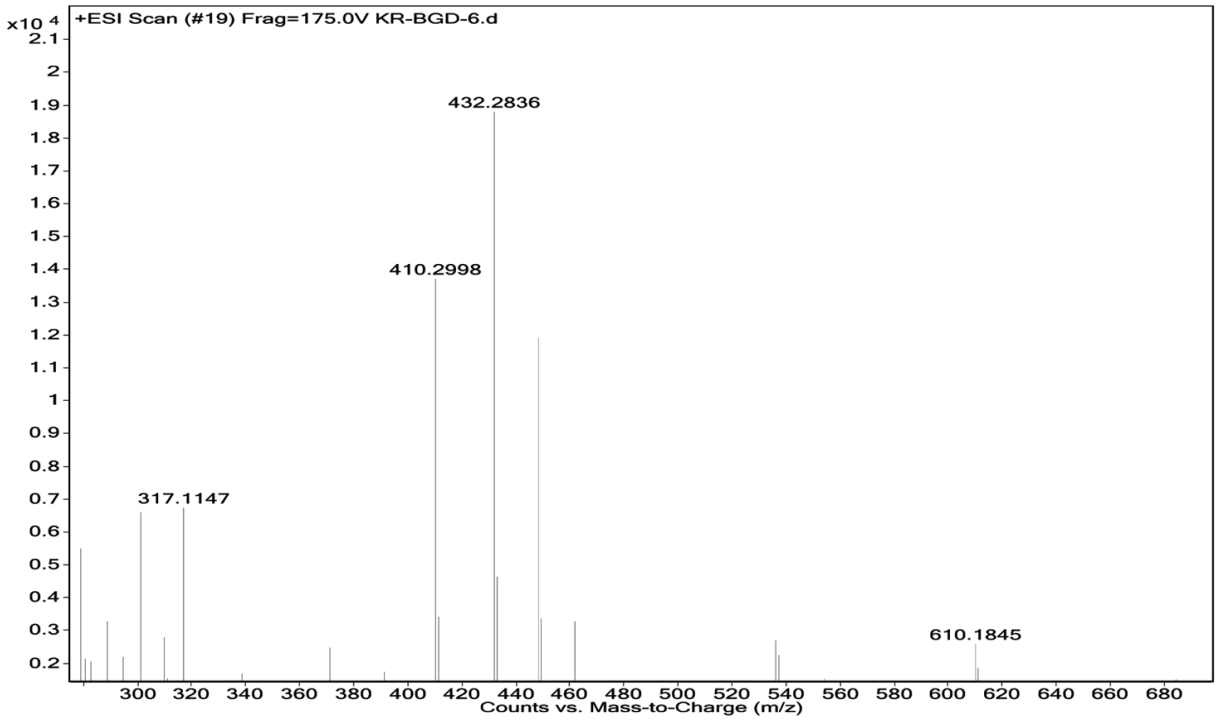

Figure S28: ESI-HRMS of M4. Mass calc. for M4: $(M+H)^+$=410.2974 Da; Mass obs.:$(M+H)^+$=410.2998 Da.

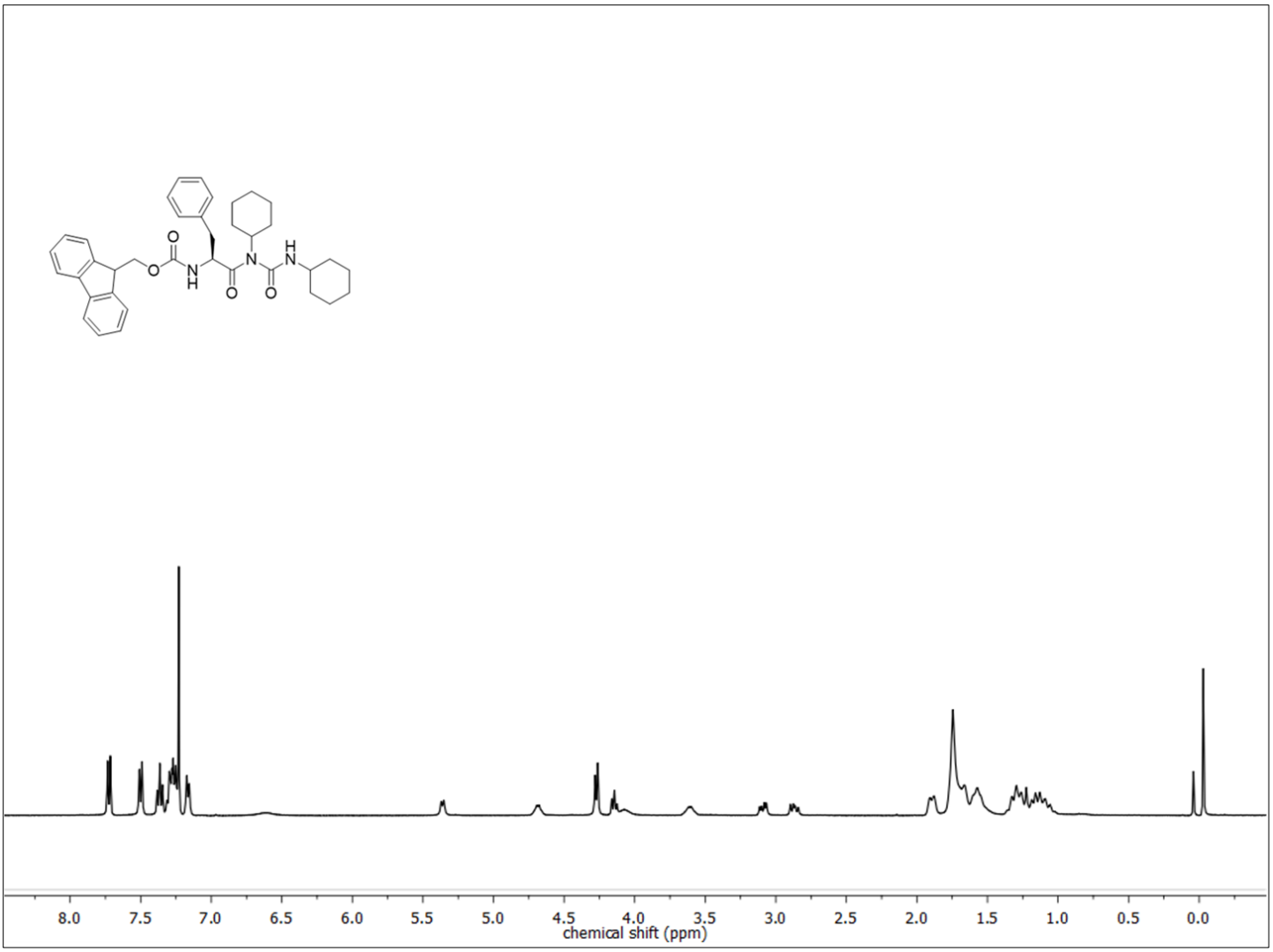

Figure S29: 400 MHz ^{1}H NMR spectra of M1 in $CDCl_3$ at 300K.

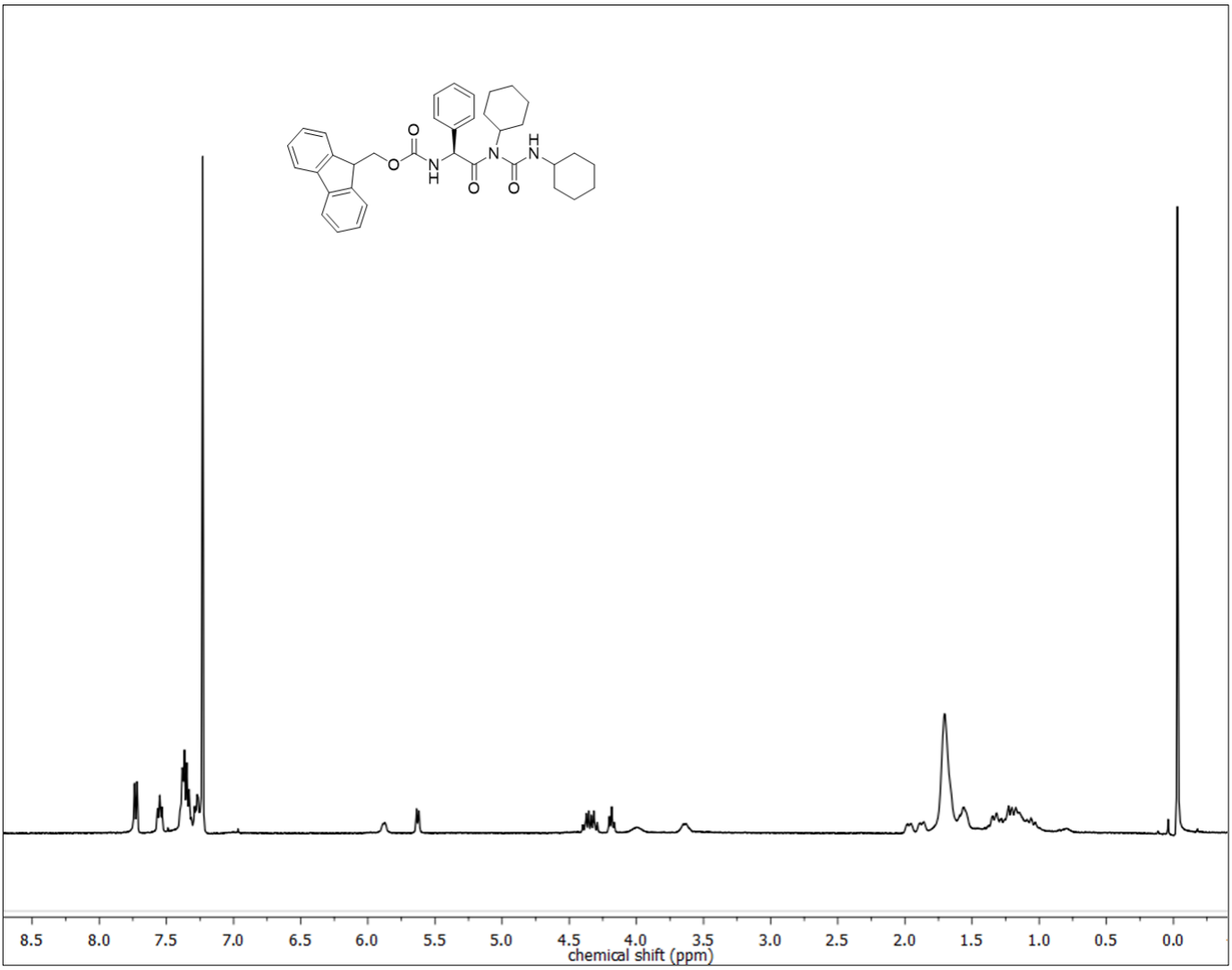

Figure S30: 400 MHz ^{1}H NMR spectra of M2 in $CDCl_3$ at 300K.

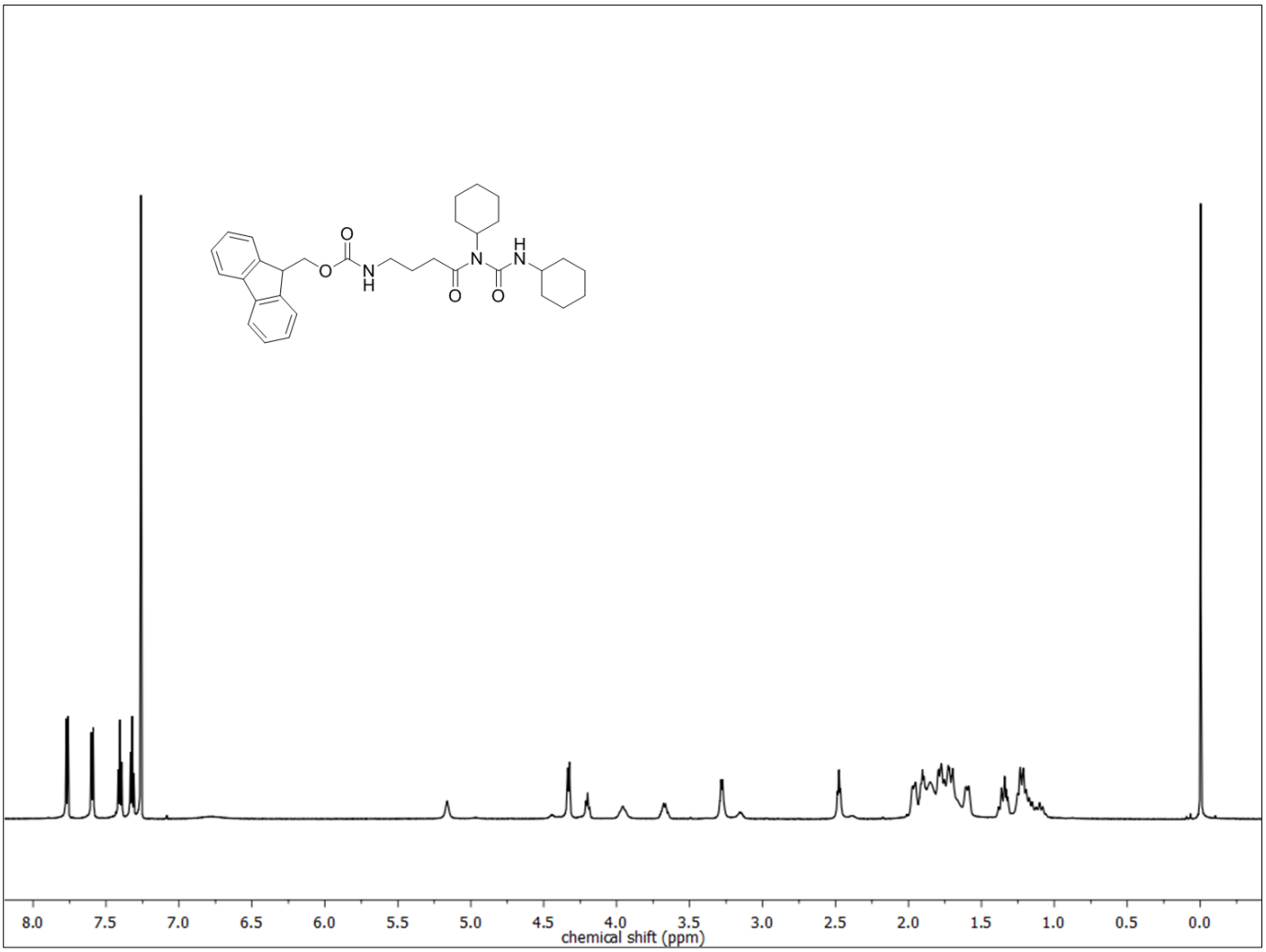

Figure S31: 600 MHz ^{1}H NMR spectra of M3 in $CDCl_3$ at 300K.

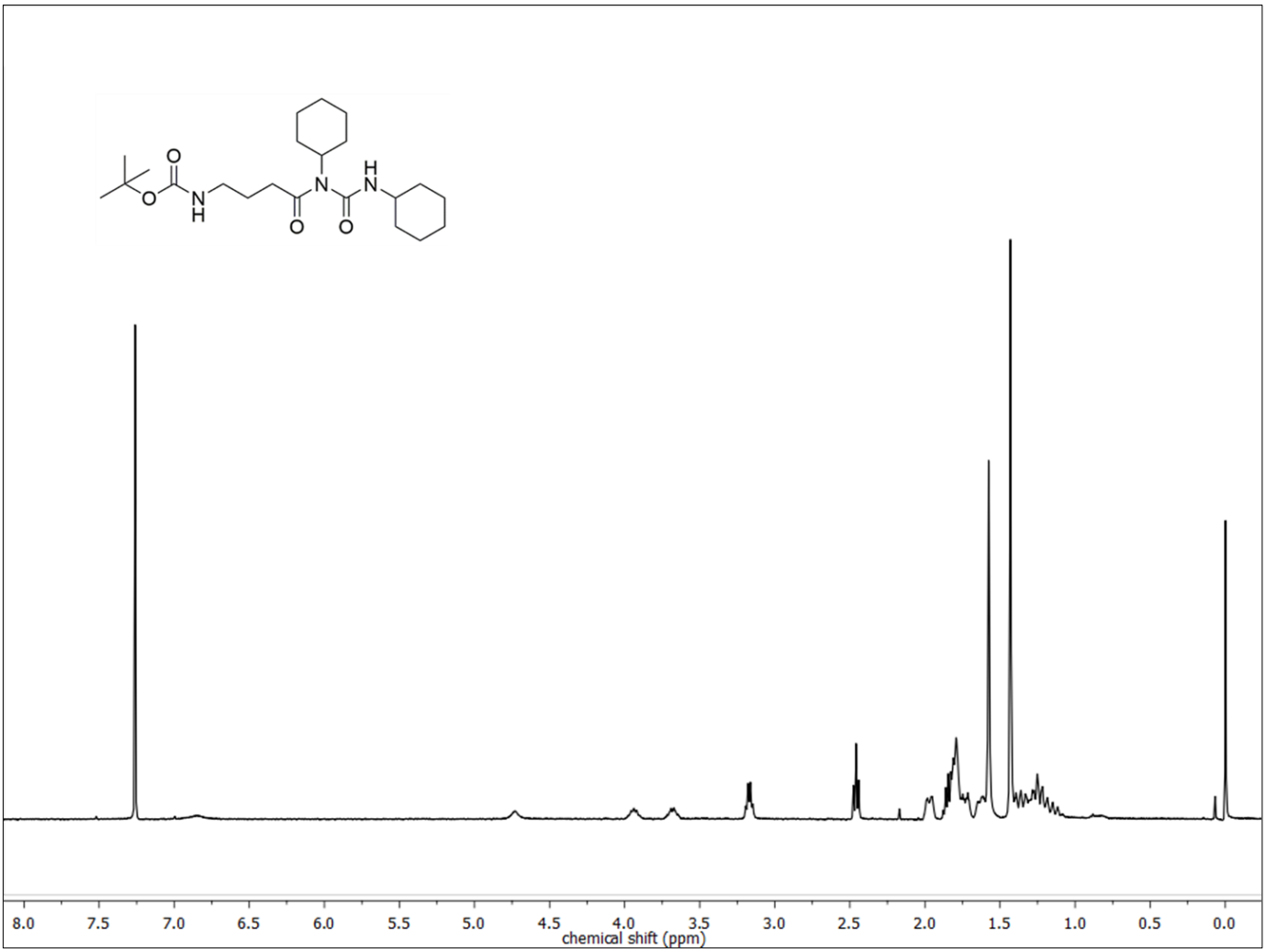

Figure S32: 400 MHz ^{1}H NMR spectra of M4 in $CDCl_3$ at 300K.

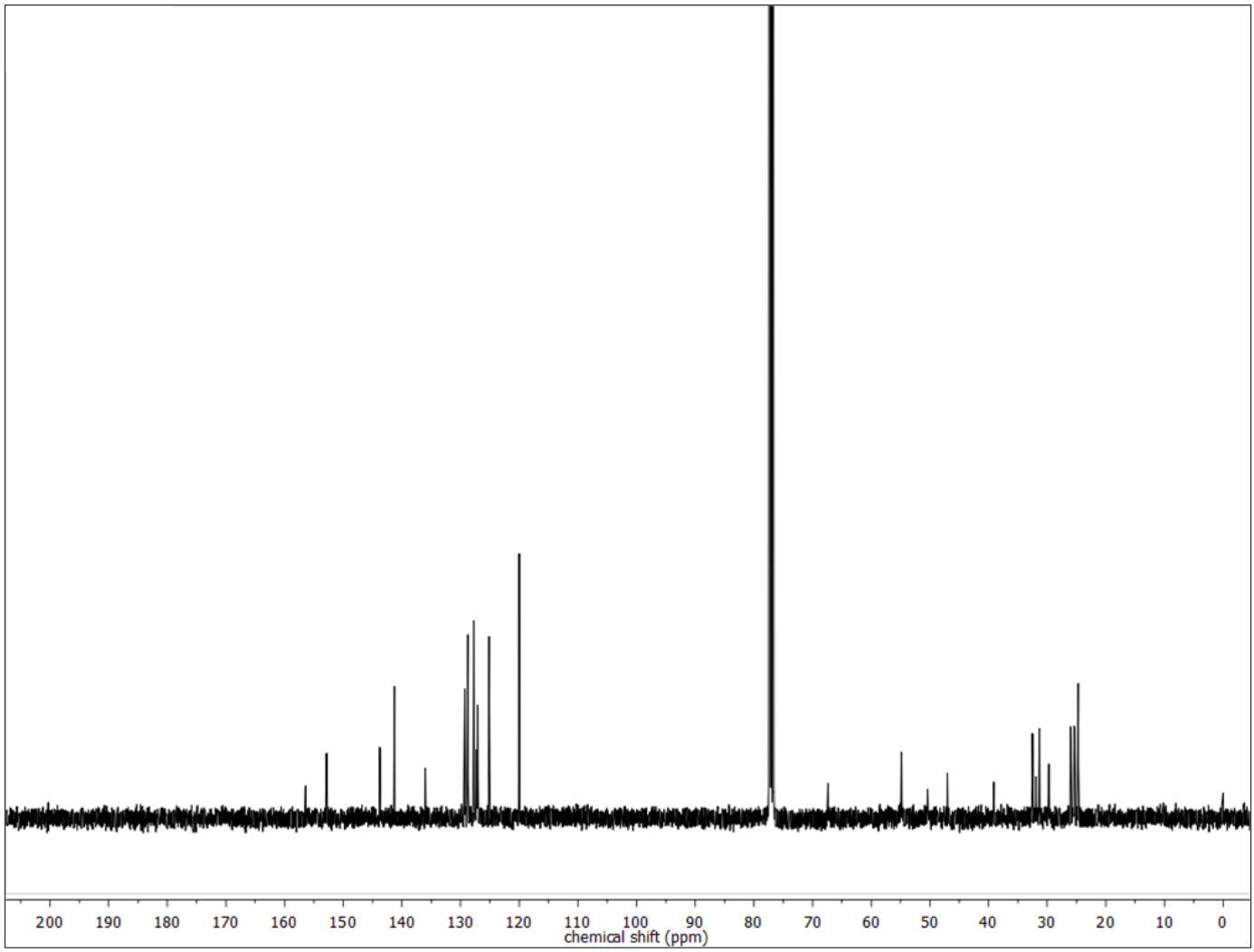

Figure S33: 400 MHz ^{13}C NMR spectra of M1 in $CDCl_3$ at 300K.

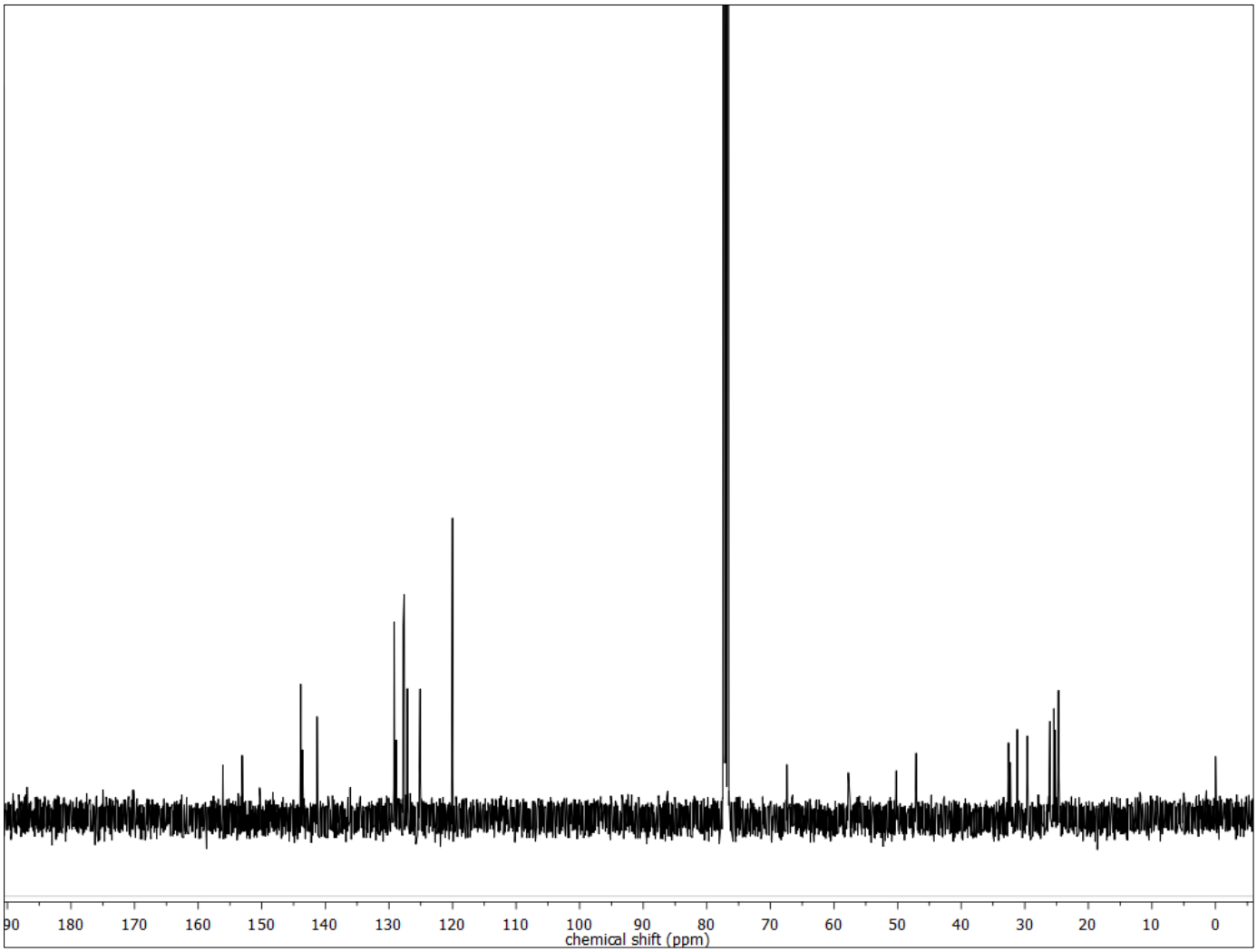

Figure S34: 400 MHz ^{13}C NMR spectra of M2 in $CDCl_3$ at 300K.

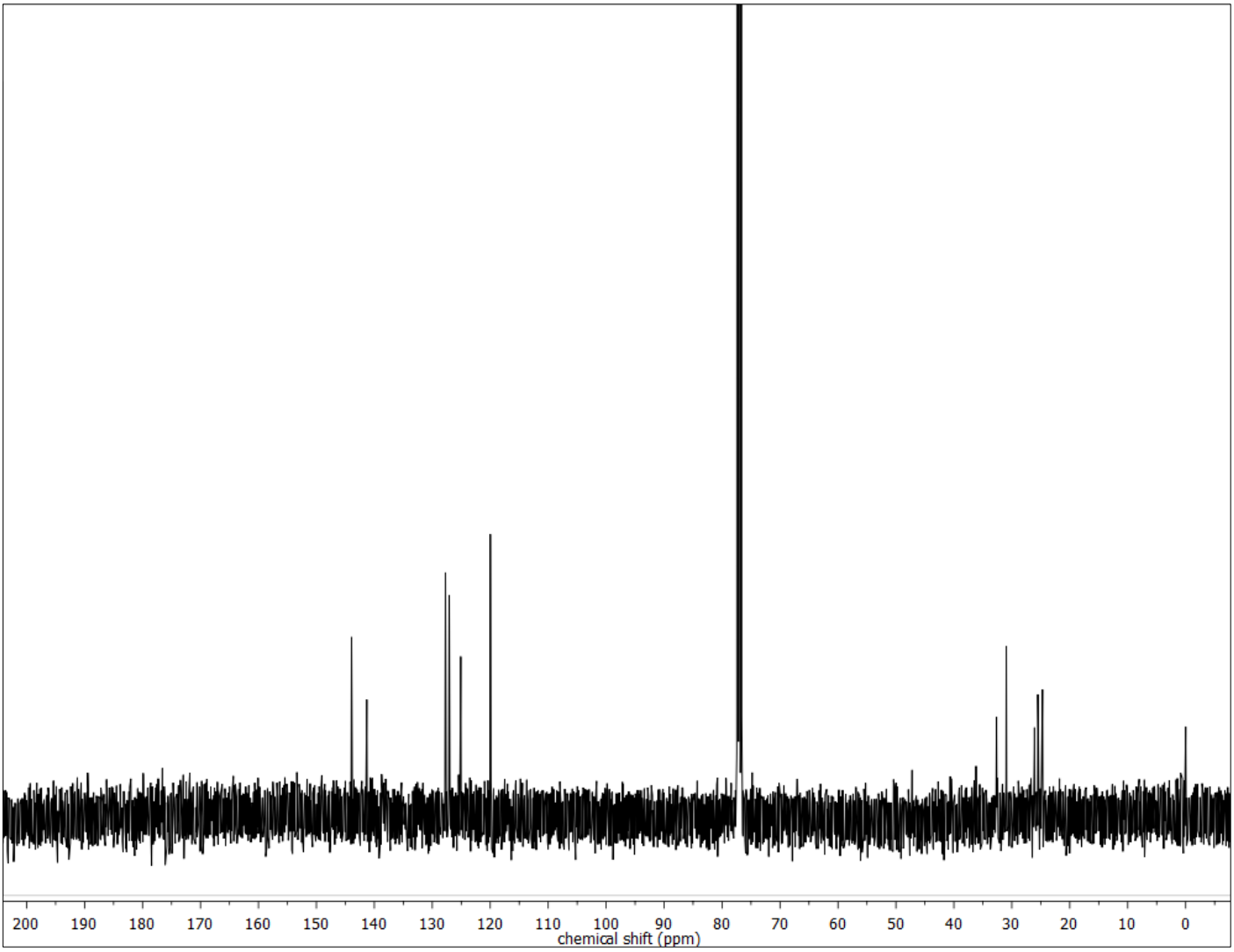

Figure S35: 400 MHz ^{13}C NMR spectra of M3 in $CDCl_3$ at 300K.

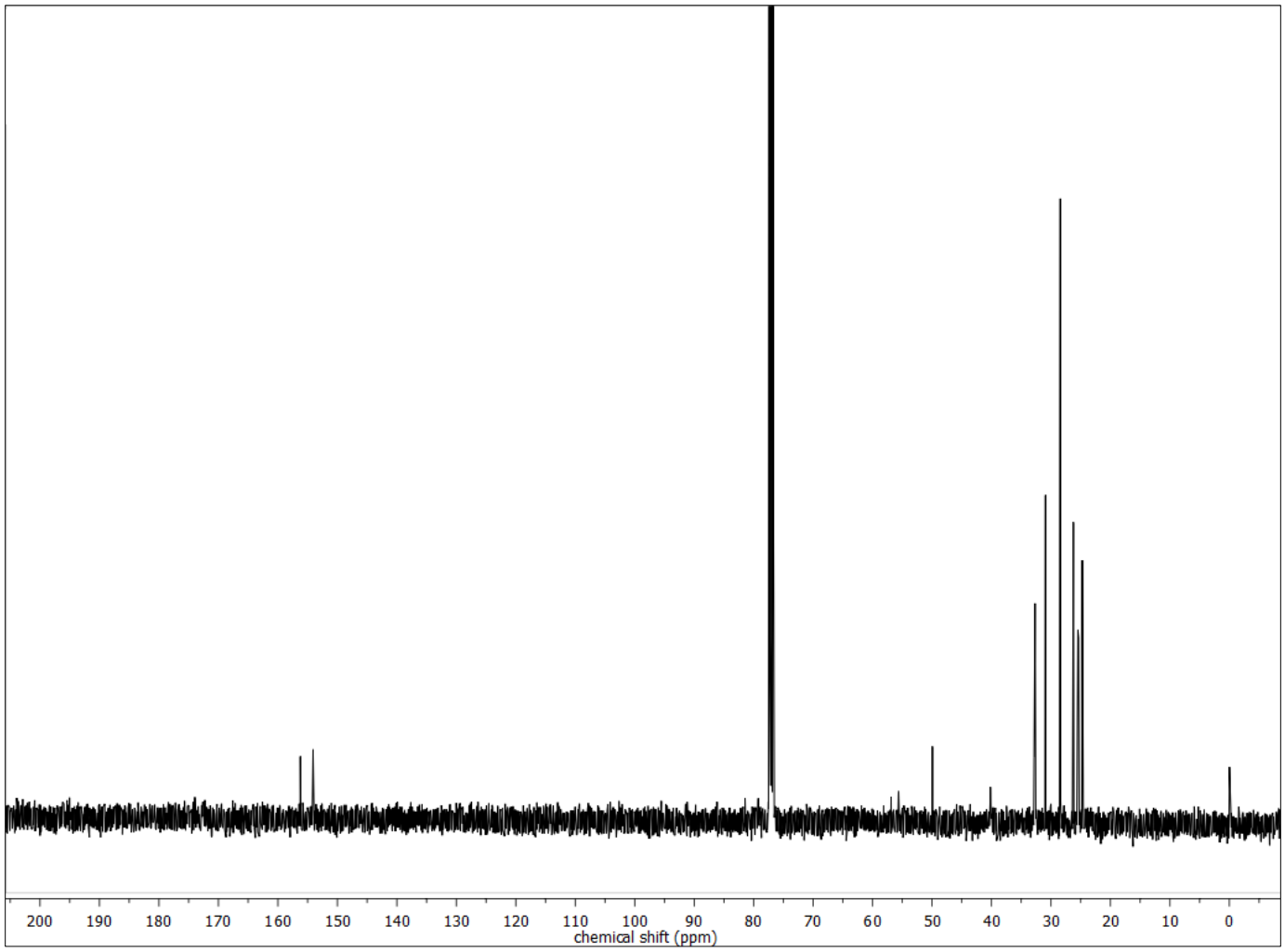

Figure S36: 400 MHz ^{13}C NMR spectra of M4 in $CDCl_3$ at 300K.

Table S1: Parameters (2θ and interplaner distance (d)) obtained from PXRD experiment on the xerogels obtained from M1-M3.

Xerogels	Peak 1		Peak 2		Peak 3		Peak 4	
	2θdegr)(ee	d(Å)	2θdegr)(ee	d(Å)	2θdegr)(ee	d(Å)	2θdegre)(e	d(Å)
M1	13.961	6.33	16.761	5.29	18.561	4.78	21.781	4.08
M2	14.521	6.11	17.221	5.16	18.901	4.69	21.881	4.07
M3	14.341	6.18	17.121	5.18	18.941	4.68	21.901	4.06

Table S2:Absorption/Loading efficiency of different dyes in organogels formed from M1-M3.

Gelators	**CV** (%)	**RB**(%)	**NR**(%)
M1	90.03	98.46	83.00
M2	87.70	97.24	92.84
M3	95.03	97.54	96.69

Table S3: Rheology parameters G´ and G´´ as a function of % strain and the nature of the gel.

Organogels	G´ (Pa)	G´´ (Pa)	% strain	Nature of the gel
M1	14409	1446.9	0.101	Strong gel
	14322	1715.1	0.793	Soft gel
	4171	4156	4.87	Cross over point
	1157	2643.3	7.87	No gel
M2	38421	3626	0.121	Strong gel
	37738	4252.2	0.795	Soft gel
	13016	9691.6	5.20	Cross over point
	6778	8687.1	8.91	No gel
M3	9950	1026.0	0.123	Strong gel
	9652	1032.2	0.371	Soft gel
	3384	3200.4	2.68	Cross over point
	859.6	1632.3	6.16	No gel